

GEORGE RABCHEVSKY

Prior to engaging himself in the field of applications of remote sensing to geology, Mr. Rabchevsky was studying civil engineering and architecture, paleontology and geomorphology. In 1961 he received a Bachelor of Science degree in geology from the American University and in 1963 a Master of Science degree in geology from the George Washington University. Even though his early geologic training emphasized paleontology and stratigraphy, he had an early interest in the applications of aerial photography to geologic mapping and geomorphology. For example, he prepared a photogeologic map of the Adams Run Anticline in Hardy County, West Virginia as part of his M. S. thesis. From 1963 to 1965 Mr. Rabchevsky was a graduate teaching assistant at the Cornell University. In 1965 Mr. Rabchevsky accepted a teaching position with the George Washington University and continued his doctoral program there. After successful completion of his doctoral course requirements and comprehensive examinations in 1969, Mr. Rabchevsky was awarded a Master of Philosophy degree. Presently he is working on his doctoral dissertation.

Mr. Rabchevsky has experience as a geological technician with the U. S. Geological Survey, a graduate teaching assistant with the George Washington and Cornell Universities, a free-lance scientific translator and interpreter and a faculty teaching position with the George Washington University. He is currently employed by Allied Research Associates, Inc.

At the Earth Resources Analysis Center of Allied Research Associates, Inc. at Lanham, Maryland, he is presently involved in the application of satellite photographic data to the evaluation and interpretation of terrestrial features. This work includes working with Nimbus AVCS, APT, IDCS and IR imagery and their possible utilization in Earth Resources studies. Concurrently, other satellite and aircraft observations are evaluated.

HYDROLOGIC CONDITIONS VIEWED BY THE  
NIMBUS METEOROLOGICAL SATELLITES\*

George A. Rabchevsky  
Allied Research Associates, Inc.  
8805 Annapolis Road  
Lanham, Maryland

Abstract

The unexploited value of the Nimbus meteorological sensor data relates to the satellites' ability for global, temporal, repetitive and uniform tonal and spatial coverage of the earth's surface. Examples are presented illustrating how synoptic views of large areas increase our interpretive capability and enable us to focus on large targets of interest. The effect of resolution of the Nimbus imaging systems on these observations will be discussed, together with the assessment of the areal and temporal magnitude of changes observed by these systems. Two case studies will be presented exemplifying the satellites' ability for repetitive observations enabling us to monitor phenomena under special conditions. One study deals with changes observed in the Antarctic ice conditions utilizing the Nimbus II and III television picture data. The other study deals with terrestrial changes in the Mississippi River Valley (USA) and the Niger River Valley (Africa), observed primarily in the 0.7 to 1.3 micron spectral band. The tonal variations are brought about by the soil moisture and vegetation boundary changes that correlate with the regional climatic and meteorological conditions. As a conclusion, it will be stressed that the utilization of Nimbus satellite photography for geology and other earth sciences will have to begin prior to the launch of the Earth Resources Technology Satellite (ERTS) planned by NASA for early in 1972.

1. INTRODUCTION

Since 1964, four operational Nimbus satellites have been flown successfully. Even though the satellites were designed primarily for meteorological purposes, substantial information on terrestrial features and phenomena are contained in Nimbus data. Studies of the applications for such data to terrestrial problems have been conducted on a limited scale. This paper will examine the feasibility of applying Nimbus data from the Advanced Vidicon

---

\*Adapted from Nimbus Views Hydrologic Conditions, presented at the First Western Space Congress, Santa Maria, California, 26-29 October 1970.

Camera System (AVCS), Image Dissector Camera System (IDCS) and High Resolution Infrared Radiometer (HRIR) experiments to hydrology and related studies. More in-depth research is, of course, necessary to fully substantiate the hydrologic uses of such data.

## 2. NIMBUS SATELLITE

Nimbus (Figure 1)\* was designed by NASA to be a meteorological satellite to provide global meteorological data useful for reliable, long-range weather forecasting. To accomplish this, photographic, infrared and ultraviolet measurements of the clouds, the atmosphere and the earth's surface have been collected (Figure 2).

Tables 1 and 2 present the Nimbus Satellites' launch record, experiments, and other characteristics. As it is evident from Table 2, the accidental elliptical orbit of Nimbus I was to the advantage of geoscientists. The perigee was low enough so that good resolution pictures (as high as 365 m.) were taken of various hydrologic and geologic conditions almost on a global scale. However excellent the Nimbus I imagery was, the new sensing capabilities provided by the 0.7 to 1.3 microns HRIR on Nimbus III (and the 10.5 to 12.5 microns thermal IR on the Nimbus IV) are more useful to some of the studies presented in this paper.

For more technical information on Nimbus operations and applications, the reader is referred to the following standard References, 1 through 11. The data is available from the National Climatic Center (NCC) of National Oceanographic and Atmospheric Administration (NOAA) and from National Space Science Data Center (NSSDC) of NASA. Depending on the user, the data is either free of charge or at cost for both the United States and foreign researchers.

## 3. BACKGROUND STUDIES

The usefulness of Nimbus data to hydrology is suggested in various publications (8, 12, 13, 14, 15, 16, 17). Brief analyses and more in-depth discussions on inland hydrologic conditions (18, 19, 20) and ice studies (21, 22,

---

\*All figures cited may be found at the end of this report.

TABLE 1  
NIMBUS EXPERIMENTS AND OPERATION SCHEDULE

Satellite	Launch Date	End of Regular Operations	MRIR	HRIR	AVCS	IDCS	SIRS	IRIS	APT	RTTS	THIR	MUSE	SCR	FWS	BUV	IRLS
Nimbus 1	28 Aug 1964	22 Sept 1964		●	●				●							
Nimbus 2	15 May 1966	15 May 1966	●	●	●				●							
Nimbus 3	14 Apr 1969	4 Feb 1970	●	●		●	●	●		●						●
Nimbus 4	8 Apr 1970	—				●	●	●		●	●	●	●	●	●	●

NIMBUS EXPERIMENTS

MRIR	-	MEDIUM RESOLUTION SCANNING RADIOMETER - 48 KM RESOLUTION
HRIR	-	HIGH RESOLUTION SCANNING RADIOMETER - 8 KM RESOLUTION
AVCS	-	THREE CAMERAS IN TRI-METROGON ARRAY PROVIDING 644 X 3059 KM CROSS TRACK SWATH - 0.08 TO 3.2 KM RESOLUTION
IDCS	-	DAYTIME CLOUD MAPPING; VIEWS 2576 X 2576 KM AREA PER FRAME - 3.2 KM RESOLUTION
SIRS	-	VERTICAL TEMPERATURE PROFILE; SURFACE AND CLOUD TOP TEMPERATURES
IRIS	-	VERTICAL PROFILES OF TEMPERATURE WATER VAPOR AND OZONE; SURFACE (TERRESTRIAL) COMPOSITION (8.0 TO 12.0 $\mu$ m)
APT	-	DIRECT DATA READOUT SYSTEM - 3.2 KM RESOLUTION
RTTS	-	REAL TIME TRANSMISSION SYSTEM - 3.2 KM RESOLUTION
THIR	-	DAY AND NIGHT SURFACE AND CLOUD TOP TEMPERATURES; ATMOSPHERIC WATER VAPOR MAPPING - 8 KM RESOLUTION
MUSE	-	CHANGES IN SOLAR RADIATION (UV)
SCR	-	ATMOSPHERIC TEMPERATURE PROFILE
FWS	-	ATMOSPHERIC WATER VAPOR; SURFACE (TERRESTRIAL) COMPOSITION (3.4 TO 4.0 $\mu$ m)
BUV	-	ATMOSPHERIC OZONE DISTRIBUTION
IRLS	-	DATA COLLECTED FROM PLATFORMS
●	-	NON-METEOROLOGICAL APPLICATIONS POSSIBLE
●	-	MARGINAL NON-METEOROLOGICAL APPLICATIONS
□	-	MAINLY METEOROLOGICAL APPLICATIONS

TABLE 2  
NIMBUS LAUNCH AND ORBITAL CHARACTERISTICS

	NIMBUS 1	NIMBUS 2	NIMBUS 3	NIMBUS 4
Launch Vehicle	Thor/Agena B	Thrust-Augmented Thor/Agena B	Thorad/Agena D	Thorad/Agena D
Launch Site	Western Test Range Vandenberg AFB California			
Launch Date	28 Aug 1964 00:57 PDT	15 May 1966 00:56 PDT	14 Apr 1969 11:54 PDT	8 Apr 1970 00:18 PDT
Orbit				
Apogee	931 km	1177 km	1132 km	1096 km
Perigee	422 km	1095 km	1069 km	1087 km
Period	99 minutes	108 minutes	107.29 minutes	107.12 minutes
Inclination	81° retrograde	79.9° retrograde	80.1° retrograde	99.89 retrograde

23, 24, 25, 26) have also been published. Nimbus data has not been extensively used to map snow cover distributions, snow thickness or run-off in the Northern Hemisphere primarily because the Nimbus satellites (with the exception of Nimbus I) have been launched in spring (see Table 1) and sensor operations terminated prior to the winter seasons.\*

### 3.1 AVCS and IDCS Data

The Nimbus AVCS and IDCS pictures have been used to map sea ice distribution and movement in the Arctic and Antarctic. A sampling of existing ice reconnaissance accomplishments over these polar "deserts" includes: location and observations of large tabular iceberg formation and motion; establishment of monthly Antarctic pack ice boundaries; detection and monitoring of leads (polynia) forming in the Antarctic.

Snow cover is an earth resource that has been observed from space for the past decade and will be surveyed by future satellites designed exclusively to view the earth's surface. For general information, Figure 3 illustrates a sampling of snow conditions viewed by the Nimbus satellite.

In the north-central United States, maps of snow distribution derived from meteorological satellite photography are already being used as input to operational flood forecasting (28, 29, 30, 31, 32, 33). Snow surveillance from rapid coverage of large areas and of observations regardless of the remoteness of the region, type of terrain or political boundaries may be conducted from satellites. Because snow accumulation in remote mountainous terrain is the prime source of water for much of the western United States, the advantages of remote sensing from space platforms may be of even greater significance for this part of the country.

Other applications of the Nimbus AVCS and IDCS pictures are the observations of terrestrial rivers and drainage systems, lakes and reservoirs, and marshes. The Nimbus ground resolution will not permit detailed hydrologic analyses but small scale observations are definitely feasible. A small sampling

---

\*ESSA meteorological satellites carrying the Nimbus developed AVCS camera systems have provided data for research studies of snow mapping (28, 29, 30, 31, 32, 33) and for operational application.

of such observations is illustrated in Figure 4. Similar pictures could serve as background information for planning more detailed studies.

Nimbus can also provide a basis for maps of drainage systems useful in interpretations of slope directions, regional relief, relative texture and density of the drainage, drainage patterns and geologic structures. Since absolute relief is not evident from Nimbus photographs, the drainage patterns become valuable to separate highlands from the basins. In some cases, the approximate steepness of the slopes may be inferred from the drainage pattern. Drainage patterns may also reveal bedding and tectonic lineations.

### 3.2 HRIR Data

The Nimbus nighttime HRIR also measures surface temperatures in cloud-free areas. Since different lithologies and surface covers may cool at different rates, the temperature maps may be useful to geohydrological exploration and location of areas for more efficient irrigation projects.

The Nimbus III daytime HRIR (0.7 - 1.3 micron) has opened up a new dimension to applications of Nimbus data to the earth sciences. The 0.7 to 1.3 micron band responds to reflected solar infrared energy and the observed variations in gray tones (on photofacsimiles) are, therefore, a good relative estimation of the near-IR reflectivity of the terrestrial surficial features. Examples illustrating the application of such data to the monitoring of soil-moisture/vegetation conditions will be presented later in the paper. The daytime HRIR data may also aid in the location of alluvium and sand deposits, especially in areas formerly occupied by ancient rivers and lakes.

An inherent disadvantage of the photofacsimiles is the resolution of the HRIR sensor. The average resolution on photofacsimiles is approximately 8 km. at the subsatellite point (Figure 7). On grid-print maps at one-to-one million scale, Mercator projection, the resolution decreases to about 12 km. The average Nimbus AVCS picture resolution, on the other hand, is approximately 3 km. Resolution requirements, however, vary depending on applications and the media sensed.

#### 4. NIMBUS VIEWS TERRESTRIAL HYDROLOGY

##### 4.1 Polar Ice

Nimbus I was the first weather satellite that provided daily photographic coverage of the polar regions. In cloud-free images, contrast is good for both the AVCS and HRIR polar photography. In the HRIR pictures, however, the pack ice edge is not as clearly delineated as in the AVCS (22) being rather a gradual change in brightness corresponding to the change from the warmer water to the colder ice. Nevertheless, abrupt changes are readily noticeable in the HRIR, such as at the edge of the Antarctic continent where a large temperature difference exists.

The main considerations in identifying the ice/water boundary are (a) the persistence of the ice/water boundary in successive images, (b) pattern characteristics of ice and cloud edges and (c) textural differences between the two (34). The most useful factor is the stability of the pack ice front, i. e. the front position changes little in a 24 to 96 hour period, while cloud patterns may shift rapidly in this time frame. Therefore, clouds may often be positively discriminated from ice simply by comparing location coordinates of successive frames.

Patterns and textures are also important in distinguishing between clouds and ice. Cloud fronts can be identified because of their linear orientation which often extends far beyond the normal limits of pack ice coverage. The "lumpy" characteristic of many cloud masses, may also be useful to identify them as clouds. The lumpy appearance is caused by the long shadows from the higher clouds cast on to the tops of the lower ones. Pack ice relief is normally less than 6 meters so that shadows cast should not be resolved by the satellite system.

##### Monthly Antarctic Pack Ice Boundary

A map of the average monthly pack ice boundaries from Nimbus II AVCS satellite data is illustrated in Figure 5. A similar study was conducted with the Nimbus I AVCS and HRIR data (23). In general, the determination of the average monthly pack ice boundary produced two valuable sets of information on the hydrology of ice in the Antarctic: (a) the existence of monthly changes (or a lack

of them) in the pack ice boundary and (b) the determination of total area under pack ice cover for each month. The areal extent of Antarctic pack ice is presented in Table 3. The values show a uniform monthly increase in pack ice areal extent in the Weddell Sea area from May to August. Note, however, that the circumpolar coverage is almost identical for months of July and August. Though the July-August boundary shifts considerably in places, the total area under ice cover is almost identical for both months.

To update the 1966 ice position from photographs, Figure 6 illustrates the comparative position of ice boundary as viewed by Nimbus II (1966) and III (1969) satellites. Similar ice boundary fluctuations may also be recorded in other polar regions, as for example, in Greenland and Iceland.

TABLE 3  
ANTARCTIC PACK ICE AREA AS DETERMINED FROM NIMBUS 2 AVCS

Month	Continent and Pack Ice Area (km <sup>2</sup> )	Continent Area (km <sup>2</sup> )	Pack Ice Area (km <sup>2</sup> )	Areal Coverage
May	$1.3498 \times 10^7$	$7.109 \times 10^6$	$6.388 \times 10^6$	"Slice"
June	$1.5181 \times 10^7$	$7.109 \times 10^6$	$8.071 \times 10^6$	from 50°W
July	$1.5902 \times 10^7$	$7.109 \times 10^6$	$8.792 \times 10^6$	clockwise
August	$1.6795 \times 10^7$	$7.109 \times 10^6$	$9.685 \times 10^6$	to 110°E
July	$2.9355 \times 10^7$	$1.6417 \times 10^7$	$1.2938 \times 10^7$	Circumpolar
August	$2.9372 \times 10^7$	$1.6417 \times 10^7$	$1.2955 \times 10^7$	

## 4.2 Surface Moisture and Vegetation

### Mississippi River Valley

Examination of the Nimbus III HRIR daytime (0.7 - 1.3 micron) reflectance data in the lower Mississippi River Valley during the period April-September 1969 revealed the presence of significant variations in pattern and tone. Investigation of the possible causes of the changes through literature review and verbal communications (34, 35, 48) suggests that the changes in reflectivity observed on the successive photofacsimiles (Figure 8) and computer produced grid-print maps (Figure 9) correspond primarily to decreases in soil moisture during the dry (1969) summer season. This moisture decrease affects the vegetal cover (wilted vegetation, poor crop yield) and soil texture and the radiometer, in turn, integrates those changes as higher reflectances.

The changes in the reflected solar radiation are easily seen on the photofacsimiles and may be expressed in relative quantitative terms from the grid-print maps (Figure 9). An increase in reflectance from 22 May to 9 August correlates with a decrease in rainfall in that area. A reversal to a lower relative reflectance during 12 September was a response to the moisture added to the ground in the form of rain. Based on rainfall statistics alone, and without any other ground checks, it is possible to conclude that the fluctuating reflectance patterns are mainly due to the soil-moisture, vegetation and soil texture conditions present in the heavily cultivated flood plain soils of the lower Mississippi Valley.

### The Ouachita River Flooding

Flooding conditions within the Mississippi River Valley during the spring season have also been detected by Nimbus remote sensing data. As ground-truthed an Apollo IX near-infrared picture (Figure 10), taken on 9 March 1969, showed an area of flooding along the Ouachita River near the Louisiana-Arkansas border and tonal changes between intensively cultivated land along the Mississippi River and the less intensive cultivation to the west of it.

Analysis of corrected Nimbus III HRIR grid-print reflectance values for 25 and 30 April show a similar flooding pattern along the Ouachita River (Figure 11). Heavy rainfall on 28 April possibly accounts for the lack of a re-

reflectance boundary between the two major vegetation types visible in the Apollo imagery (48).

The 6 June values suggest a reduction of the flooded area. However, a weak northeast-southwest tonal gradient corresponding to the two major vegetation types visible in the Apollo picture has now appeared.

By 9 August, there is a marked reflectance increase in the eastern half of the picture. No rain had fallen in this area in over two weeks. This drought seems to have had a pronounced effect on reflectance in the intensively cultivated area along the Mississippi River with a lesser effect on the different vegetation in the western half of the map. All evidence of the spring flood along the Ouachita River has disappeared by this date.

Even though the 12 September map indicates an overall reduction of reflectance values (due to rainfall of about one inch between 2 and 7 September), the NE-SW vegetation boundary is still evident.

There is no doubt that the Ouachita flood did occur. Not only was it picked up by the Nimbus satellite HRIR sensor, but it was also substantiated by ground-truth, in this case Apollo IX spacecraft imagery. Ground-truth, unfortunately, is not always available for the interpretation of many other remotely sensed hydrological events. The detection of the Ouachita flood on Nimbus imagery, however, offers us quasi-ground-truth for the interpretation of similar temporal reflectance patterns in other regions of the world.

### Niger River Valley

Another terrestrial event monitored by the Nimbus III HRIR and briefly described here has occurred in the vicinity of the inland "delta" of the Niger River, western Africa. Examination of a series of photofacsimile prints from June to November of 1969 revealed marked tonal changes. Additionally, evaluation of the digitized grid-print maps of the area provides quantitative information on the solar reflectance characteristics of this area.

Photofacsimile data - In general, the transitions in shades of gray from dark along the Guinea coast (Nigeria, Dahomey, Togo, etc.) to moderate gray

and finally into pale gray at approximately  $15^{\circ}$  N latitude roughly correlate with the broad vegetative zones that include tropical forest, Savannah forest and Savannah grasslands that belt the West African continent south of the Sahara Desert. The transition in IR solar reflectance intensity (expressed in gray tones on prints) is best illustrated on the November 18 nearly cloud-free image, the dry season for tropical West Africa (Figure 12). The shifting regional vegetation boundaries (gray tones) in turn correspond to changes in soil moisture, as a response to the meteorological conditions, are partly illustrated in Figure 11.

A more local ground event is illustrated in Figure 13. The dark pendulous shaped area with its associated side lobes is the great interior "delta" (Pleistocene) of the Niger River. Parts of this region, particularly between Lakes Faguibine and Haribongo, are striated by broadly separated linear dunes of stabilized sand that generally trend northeasterly. Drainage in this region follows the interdune areas that are, in places, several miles wide (Figure 14). The areal, tonal and temporal changes illustrated in Figure 10 most likely correspond to the changing hydrologic and vegetative conditions on the ground. Since Nimbus III HRIR daytime channel senses reflected solar radiation in the 0.7 to 1.3 micron band range, surface water and vegetation absorb more solar radiation than most bare surfaces or dry sands. The increases in the darker tones, therefore, may indicate an increase in soil-moisture content, spread of a denser vegetal cover, local flooding or an increase in evapotranspiration.

A cursory literature examination of ground conditions present in the Niger River Valley south of Timbuktu support the explanation presented above. Table shows the increase of monthly rainfall in the area from April to December. On HRIR imagery reflectances began to drop off sharply in June to August and continued to decrease until their lowest values in October and November. The great volume of water (May to October) inundates the Niger River "delta" (interconnected swamps and lakes) and is partly soaked up by the soil and partly evaporates. The increased ground moisture, in turn, gave rise to the luxuriant vegetal growth as inferred from the varying regional reflectance patterns. It is interesting to note that the Kainje reservoir above Bussa (Nigeria), the Akasombo reservoir on the Volta River, Lake Chad, the inland "delta" of the Niger River above Mopti including Lake Faguibine and Lake Haribongo, and some segments of the Niger River can be delineated with a moderate degree of confidence on the October and

TABLE 4: MONTHLY RAINFALL (mm.)  
IN THE NIGER RIVER HEADWATERS  
MALI, WEST AFRICA (47)

STATION	MONTH								
	APRIL	MAY	JUNE	JULY	AUG.	SEPT.	OCT.	NOV.	DEC.
BAMA KO	3	54	104	236	276	160	129	0	0
BOUGOUNI	24	42	177	300	189	245	139	13	0
SEGOU	0	33	90	170	169	152	72	0	0
MOPTI	0	4	22	141	268	56	25	0	0
TIMBUKTU	0	1	0	95	9	37	5	0	0

November imagery despite the fact that this period marks the beginning of the "harmattan" season when the atmosphere inland is ordinarily very dusty and hazy to altitudes of about 3050 m. (40).

Furthermore, the varying pendulous-shaped area, repetitively observed on Nimbus imagery corresponds primarily to the Quaternary and Tertiary sediments underlying the flood plain of this "delta" (Figure 15). And since these sediments are made up of hydromorphic (waterlogged) soils and lacustrine and riverine alluvium (41, 45), their water retention capacity is high. The stored ground water, in turn, supports vegetation growth, to a degree directly proportional to the water capacity. The apparent time lag in the vegetal response to the moisture saturation of soil explains why the "delta" area reflects solar radiation more during the maximum rainfall (July-August) and is at its minimum at the beginning of the dry season (November).

The remote monitoring by Nimbus of a "flood" in the Niger River Valley, may also be indirectly substantiated by the fact that the surrounding area is

marshy and subject to periodic flooding (42).

HRIR digitized data - The Nimbus daytime HRIR data may also be displayed on computer produced grid-print maps. Figures 16 and 17 illustrate the distribution of reflectance patterns in the Niger River Valley expressed in quantitative values. The values have been contoured automatically and then enhanced manually. Notice the gross regional shifts of tonal changes (reflectance values) brought about by seasonal conditions. The reflectance values below 10% shift from approximately 12° and 13° latitude on Figure 13A (July), to 15° and 16° latitude on Figure 13B (August), and Figure 17 (November).

In general, the 7-9% reflectance values over continental areas are indicative of "normal" ground conditions, i. e. moisture stored in the "B" and "C" soil horizons supporting vegetal growth in the "A" horizon. This obviously does not apply to regions underlain by dark colored lithologies, as for examples, lava flows, coal, bituminous limestone, etc. Reflectances below 5-6% are, in turn, correlated with water bodies or extremely hydrous soils (Figure 17). Sands and clouds usually respond with reflectances above the 10-12% values.

Due to the Nimbus HRIR sensor resolution, however, these reflectance value boundaries fluctuate depending on the size and position of water bodies, the time of the year, and the viewing angle. Furthermore, the sensitivity of the HRIR sensor seems to degrade with time, so that progressively somewhat lower reflectances recorded on digitized maps are not necessarily correlative with ground conditions.

A more localized and intriguing reflectance pattern appears in the northwest quadrant of Figure 16. This pronounced NW-SE trending subelongate pattern does not always occur, however, on all maps, but seems to appear only after periods of regional rainfall. It may be that this is caused by the run-off being stored in the more porous soils or alluvium; the soil-moisture thus giving rise to the anomalous reflectance pattern. This, however, does not explain completely the reoccurrence of this pattern on different maps. It is hypothesized, therefore, that this feature may represent the ancient course of the Niger River (49). The existence of a former route of the Niger River is not new (50). The significance of this interpretation, however, is in the probable ability of the satellite remote sensors to detect such obscure terrestrial features. The applications of such observations are, of course, obvious and hopefully will

materialize with the initiation of the acquisition of higher resolution imagery from the planned Earth Resources Technology Satellites.

## 5. CONCLUSIONS AND RECOMMENDATIONS

The foregoing discussion presented a brief look into the feasibility of utilizing Nimbus photographs and imagery for hydrology oriented studies and applications. The value of such data is not just the ability of the Nimbus sensors to pick out local hydrologic features, but also their ability to provide geoscientists with repeated global and synoptic observations. The fact that regional soil-moisture and vegetative changes were observed from an altitude of 966 km. in Mississippi and Niger River Valleys indicates the usefulness of Nimbus data for regional hydrological and ecological projects. In the Antarctic and Arctic Seas, the importance of satellite data for ice hydrology and for near real-time evaluation of ship routing (36, 37, 38, 39) has been expressed repeatedly.

The Earth Resources Technology Satellite (ERTS) is planned for launch by NASA for 1972. The expected repeat coverage from ERTS will enable us to map dynamic terrestrial surface conditions (coastal processes, snowfall and run-off, flooding and drought, vegetation bloom) and classify events and landforms (lakes, rivers, deltas, geologic structures and hazards) on a regional scale for the first time. The presently available Nimbus satellite repeat observations data, therefore, may generate background studies for future more detailed and local applications of the ERTS photographs and imagery.

The following is a tentative list of possible hydrologically oriented studies that may be conducted with the Nimbus data:

1. Monitor regional soil-moisture and vegetation conditions (floods and droughts).
2. Determine the occurrence and areal changes of snow cover in mountainous areas.
3. Correlate snow line changes with snow-melt and subsequent run-off in large watersheds.
4. Surveillance of freeze-up and break-up of sea-ice for charting of shipping lanes.

5. Track movement of large icebergs for warnings to sea traffic and sea-mining operations.
6. Monitor albedo of the Arctic ice during periods of maximum change (June through August).
7. Monitor areal extent and fluctuations of the Antarctic and Greenland ice caps.
8. Monitor and classify ice concentrations and large floes in sea ice.
9. Develop techniques to enhance snow and ice texture information available on the direct read (APT) photographic and IR data.
10. Develop new classification systems (numerical, optical or geometrical) for lakes and drainage basins using large area coverage photos and imagery.

DEFINITIONS AND ACRONYMS

- "A" soil horizon - the upper part of soil. It consists of mineral layers of maximum organic accumulation.
- Albedo - the percentage of the incoming radiation that is reflected by a natural surface such as the ground, ice, snow, or water.
- Alluvium - a general term for all detrital deposits resulting from the operations of modern rivers, thus including the sediments laid down in river beds, flood plains, lakes, fans at the foot of mountain slopes, and estuaries. Alluvium may become lithified, as has happened frequently in the past, and then may be termed ancient alluvium.
- Apogee - the point in an orbit which is furthest from the center of the earth.
- APT - Automatic Picture Transmission.
- AVCS - Advanced Vidicon Camera System.
- "B" soil horizon - lies under (below) the "A" horizon. It consists of weathered material with an accumulation of clay, iron, or aluminum, or with more or less blocky or prismatic structure.
- BUV - Backscatter Ultraviolet Spectrometer.
- "C" soil horizon - the "C" horizon, under the "B" horizon, is the layer of unconsolidated, weathered parent material.
- Data orbit - the orbit during which data were acquired by the satellite.
- Degradation - the lessening of image quality because of noise or any optical, electronic, or mechanical distortions in the image-forming system.
- ERTS - Earth Resources Technology Satellite.
- ESSA - Environmental Science Services Administration.
- Evapotranspiration - a term embracing that portion of the precipitation returned to the air through direct evaporation or by transpiration of vegetation, no attempt being made to distinguish between the two.
- Ferruginous (furruginous) - of, pertaining to, or containing iron.
- Floe - mass of floating ice some 30 meters to 8 km. across not fast to any shore, formed by breaking up of the frozen surface of a large body of water.

- Flood plain - that portion of a river valley, adjacent to the river channel, which is built of sediments during the present regimen of the stream and which is covered with water when the river overflows its banks at flood stages.
- FWS - Filter Wedge Spectrometer.
- Grid-print maps - computer produced maps of temperature or reflectance values.
- Harmattan - a dust-laden land wind on the Atlantic coast of Africa in certain seasons.
- HRIR - High Resolution Infrared Radiometer.
- Hydrous (hydromorphic) - containing water chemically combined, as in hydrates.
- IDCS - Image Dissector Camera System.
- Imagery - the pictorial representation of a subject produced by electromagnetic radiation emitted or reflected from a subject, or transmitted through the subject, and detected by a reversible-state physical or chemical transducer whose output is capable of providing an image.
- Infrared - pertaining to or designating the portion of the electromagnetic spectrum with wavelengths just beyond the red end of the visible spectrum, such as radiation emitted by a hot body. Invisible to the eye, infrared rays are detected by their thermal and photographic effects. Their wavelengths are longer than those of visible light and shorter than those of radio waves, light rays whose wavelength is greater than 700 milli-microns.
- IR - infrared.
- IRIS - Infrared Interferometer Spectrometer.
- IRLS - Interrogation Recording and Location System.
- Lacustrine - of, or pertaining to, or formed or growing in, or inhabiting, lakes.
- Large scale - a large scale map shows a small area of the surface of the earth and with great detail.
- Mercator map projection - a conformal map projection of the so-called cylindrical type.
- Micron - a unit of length equal to the one one-millionth of a meter.
- MRIR - Medium Resolution Infrared Radiometer.
- MUSE - Monitor of Ultraviolet Solar Energy.
- NASA - National Aeronautics and Space Administration.
- Nimbus - an experimental meteorological earth orbiting satellite.
- Pack ice - any large area of floating ice consisting of pieces of ice driven closely together.

- PDT - Pacific Daylight Time.
- Perigee - the point in an orbit which is nearest the center of the earth.
- Photofacsimile - a pictorial (photographic) representation of temperature or reflectance values.
- Photography - the mapping or surveying of terrain by means of photography. The production of a permanent or ephemeral image of a subject on a medium which is directly exposed to electromagnetic radiation emitted or reflected from the subject, or transmitted through the subject, and is affected by the radiation in direct proportion to the emission, reflection, or transmission characteristics of the subject.
- Polynia - a space of open water in the midst of ice.
- Porous - containing voids, pores, interstices, or other openings which may or may not interconnect.
- Quaternary - the younger of the two geologic periods or systems in the Cenozoic era.
- Radiometer - a radiation measuring instrument having substantially equal response to a relatively wide band of wavelengths in the infrared region. Radiometers measure the difference between the source radiation incident on the radiometer detector and a radiant energy reference level.
- Regional - extending over large areas in contradiction to local or restricted areas.
- Remote sensing - in simplest terms, remote sensing is the detection and/or evaluation of objects without direct contact. In a restrictive sense, remote sensing activities include only those involving the detection of the electromagnetic radiant energy.
- Resolution - the minimum distance between two adjacent features, or the minimum size of a feature, which can be detected by a photographic or an imaging system. For photography, this distance is usually expressed in line pairs per millimeter recorded on a particular film under specified conditions; as displayed by radar, in lines per millimeter. If expressed in size of objects or distances on the ground, the distance is termed ground resolution.
- Retrograde orbit - an orbit with an inclination angle between  $90^{\circ}$  and  $180^{\circ}$ , i. e. the satellite has a westward component of motion.
- Riverine - pertaining to a river.

RTTS - Real Time Transmission System.

SCR - Selective Chopper Radiometer.

SIRS - Satellite Infrared Spectrometer.

Small scale - a small scale map presents only general features. It covers a large area of the earth, but shows little detail.

Spectral band - an interval in the electromagnetic spectrum defined by two wavelengths, frequencies, or wave numbers.

Subsatellite point - intersection of the local vertical through the satellite with the earth's surface, with the image plane, or with the celestial sphere.

Tertiary - the earlier (older) of the two geologic periods comprised in the Cenozoic era, in the classification generally used. Also, the system of strata deposited during that period.

THIR - Temperature Humidity Infrared Radiometer.

Vidicon - television camera tube.

REFERENCES

1. General Electric, January 1970: Nimbus IV Reference Manual, Space Division, Valley Forge Space Center.
2. General Electric, 1969: Nimbus III Reference Manual, Space Division, Valley Forge Space Center.
3. National Aeronautics and Space Administration, 1965: Nimbus I High Resolution Radiation Data Catalog and Users' Manual, Goddard Space Flight Center, prepared by Allied Research Associates, Inc.
4. National Aeronautics and Space Administration, 1965: Nimbus I Users' Catalog: AVCS and APT, Goddard Space Flight Center, prepared Allied Research Associates, Inc.
5. National Aeronautics and Space Administration, 1966: Nimbus II Users' Guide, Goddard Space Flight Center, prepared by Allied Research Associates, Inc.
  - , 1966: The Nimbus II AVCS World Montage Catalog.
  - , 1966: The Nimbus II HRIR Montage Catalog.
  - , 1967: The Nimbus II MRIR Catalog, Vol. I and II.
  - , 1966: The Nimbus II Data Catalog, Vol. I, II, III, IV and V.
6. National Aeronautics and Space Administration, 1969: The Nimbus III Users' Guide, Goddard Space Flight Center, prepared by Allied Research Associates, Inc.
  - , 1969: The Nimbus III Catalog, Vol. I, Part 1 and 2.
  - , 1969: The Nimbus III Data Catalog, Vol. II and III.
7. National Aeronautics and Space Administration, 1970: The Nimbus IV Users' Guide, Goddard Space Flight Center, prepared by Allied Research Associates, Inc.
8. Sabatini, R. and J. Sissala, 1968: Project NERO--Nimbus Earth Resources Observations, Tech. Rept. No. 7, Contract No. NAS 5-10343, Allied Research Associates, Inc.
9. Greaves, J. R., J. H. Willand and D. T. Chang, 1968: Observation of Sea Surface Temperature Patterns and Their Synoptic Changes Through Optical Processing of Nimbus II Data, Final Report, Contract No. NASW-1651, Allied Research Associates, Inc.

10. Kreins, E. R. and L. J. Allison, 1969: Color Enhancement of Nimbus High Resolution Infrared Radiometer Data, Goddard Space Flight Center, NASA Publication X-622-69-86.
11. Demaso, J. M., R. P. Rappaport and A. Ruiz, 1969: A Digital Color Printer, presented by Allied Research Associates, Inc. at the Electro-Optical Systems Design Conference, New York.
12. Rabchevsky, G., 1970: Comments on the Geologic Use of Nimbus I Television Photography, Proceedings of the First Western Space Congress, Vandenberg Scientific and Technical Societies Council, Santa Maria, California.
13. Conti, M. A., 1967: Evaluation of Nimbus High Resolution Infrared Radiometer (HRIR) Imagery, U. S. Geological Survey, Open File Report.
14. Neal, J. T., Capt., USAF, 1968: Playa Surface Morphology, Misc. Inv., AFCRL, Environmental Research Paper No. 283, Terrestrial Sciences Lab, Project No. 8623.
15. Kuers, G., 1968: Interpretation of Daytime Measurements by the Nimbus I and II HRIR, NASA Publication TN D-4552.
16. MacLeod, N. H., 1970: Ecological Interpretation of Nimbus III HRIR Data, Goddard Space Flight Center, NASA Publication X-652-70-98.
17. Widger, W., J. Barnes, E. Merritt and R. Smith, 1965: Meteorological Interpretation of Nimbus High Resolution Infrared (HRIR) Data, Final Report, Contract No. NAS 5-9554, republished as NAS CR-352, Allied Research Associates, Inc.
18. Hahl, D. C. and A. H. Handy, 1966: Hydrologic Interpretation of Nimbus Vidicon Image--Great Salt Lake, Utah, U. S. Geological Survey, Open File Report.
19. Pouquet, J., 1969: Possibilities for Remote Detection of Water in Arid and Sub-arid Lands Derived from Satellite Measurements in the Atmospheric Window 3.5 - 4.2 Microns, paper presented at the International Conference on Arid Lands in a Changing World, Tucson, Arizona.

20. Nordberg, J. and R. E. Samuelson, 1965: Terrestrial Features Observed by the High Resolution Infrared Radiometer in Observations from the Nimbus I Meteorological Satellite, NASA Publication SP-89, pp. 37-59.
21. Sissala, J., 1969: "Observations of An Antarctic Ocean Tabular Iceberg from the Nimbus II Satellite", Nature, Vol. 224, pp. 1285-1287.
22. Popham, R. and R. E. Samuelson, 1965: Polar Exploration with Nimbus in Observations from the Nimbus I Meteorological Satellite, NASA Publication SP-89, pp. 47-49.
23. Predoehl, M., 1966: "Antarctic Pack Ice Boundaries Established from Nimbus I Pictures", Science, Vol. 153, pp. 861-863.
24. Barnes, J. C., D. T. Chang and J. H. Willand, 1969: Use of Satellite High Resolution Infrared Imagery to Map Arctic Sea Ice, Document No. 8G60F (Final Report, Contract No. N62306-68-C-0276, NASA/NAVOCEANO Spacecraft Oceanography Project), Allied Research Associates, Inc.
25. Bowley, C. J., 1969: Use of Nimbus II APT to Determine the Rate of Ice Disintegration and Dispersion in Hudson Bay, Tech. Rept. No. 8, Contract No. NAS 5-10343, Allied Research Associates, Inc.
26. Knapp, W. W., 1969: "A Satellite Study of the Ice in Antarctic Coastal Waters", Antarctic Journal, Sept.-Oct. 1969, pp. 222-223.
27. Lowman, P. O., Jr., 1967: Geologic Applications of Orbital Photography, NASA, Tech. Note TN D-4155.
28. Popham, R. W., A. F. Flanders and H. Neiss, 1966: Second Progress Report on Satellite Applications to Snow Hydrology, Proceedings of 23rd Annual Meeting, Eastern Snow Conference, Hartford, Conn.
29. Barnes, J. C. and C. J. Bowley, 1966: Snow Cover Distribution As Mapped from Satellite Photography, Final Report, Contract No. CWB-11269, Allied Research Associates, Inc.
30. Barnes, J. C. and C. J. Bowley, 1968: Operational Guide for Mapping Snow Cover from Satellite Photography, Final Report, Contract No. E-162-67(N), Allied Research Associates, Inc.

31. Barnes, J. C. and C. J. Bowley, 1968: "Snow Cover Distribution as Mapped from Satellite Photography", Water Resources Research, 4, (2), pp. 257-272.
32. Barnes, J. C., 1969: Satellite Surveillance of Mountain Snow in the Western United States, Final Report, Contract No. E-196-68, Allied Research Associates, Inc.
33. Barnes, J. C. and C. J. Bowley, 1970: The Environmental Satellite Data for Mapping Annual Snow-Extent Decrease in the Western United States, Final Report, Contract No. E-252-69(N), Allied Research Associates, Inc.
34. Sissala, J., 1970: Personal Communique.
35. Palmer, W. C., 1970: Personal Communique.
36. Gibbs, M. E., 1968: The Utilization of Meteorological Satellite Data in Antarctica, U. S. Naval Support Force--Antarctica, Washington, D. C.
37. Freeman, R. F., 1968: Use of Satellite Data at Kodiak in Proceedings, Sea Ice Conference, U. S. Fleet Weather Facility, Navy Department, Suitland, Maryland.
38. Whittman, W. I., 1968: Satellite Imagery in Proceedings, Sea Ice Conference, U. S. Fleet Weather Facility, Navy Department, Suitland, Maryland.
39. Popham, R. W., 1968: Sea Ice Conference Summarizing and Future Outlook in Proceedings, Sea Ice Conference, U. S. Fleet Weather Facility, Navy Department, Suitland, Maryland.
40. Phoenix, D., 1970: Personal Communique.
41. D'Hoore, J. L., 1964: Soil Map of Africa, Scale 1/5,000,000, Commission for Technical Cooperation in Africa, Joint Project No. 11, Publication No. 93.
42. Dalrymple, R. G., 1970: Cartographic Applications of Orbital Photography, NASA Publication X-644-70-110.
43. Environmental Science Services Administration, 1969: Climatological Data, Environmental Data Service, U. S. Department of Commerce.
44. National Aeronautics and Space Administration, 1968: Earth Photographs from Gemini VI through XIII, Scientific and Technical Information Division, Office of Technology Utilization.

45. Association des Services Geologiques Africains (A.S.G.A.), 1963: Geological Map of Africa, co-edition A.S.G.A. and U. N. Educational Scientific and Cultural Organization (UNESCO).
46. Thoren, R., 1969: Picture Atlas of the Arctic, Elsevier Publishing Company.
47. Environmental Science Services Administration, 1969: World Weather Data Center A, Foreign Data Station, Ashville, North Carolina.
48. Sissala, J. and G. Rabchevsky, 1970: Terrestrial Changes Monitored by the Nimbus Meteorological Satellites, Proceedings of the First Western Space Congress, Santa Maria, California, October 1970.
49. Pouquet, J. and G. Rabchevsky, 1970: The Niger (Africa) Interior Delta (Macina) Remotely Sensed by the Nimbus II and III Satellite HRIR Daytime and Nighttime Radiometers, Allied Research Associates, Inc., unpublished in-house report.
50. McGinnies, W. G., B. J. Goldman and P. Paylore, 1970: Deserts of the World, The University of Arizona Press.

## NIMBUS IV

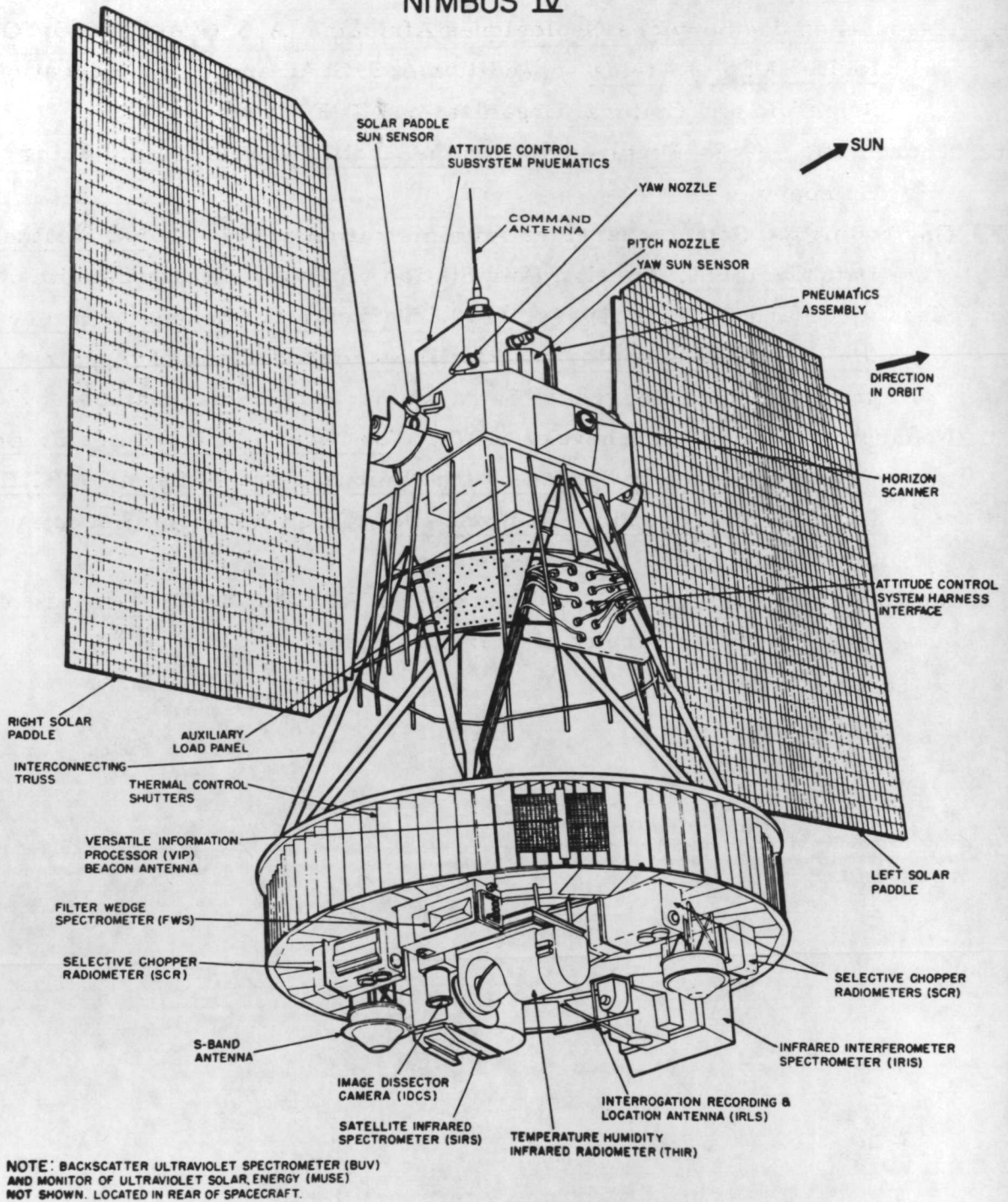


Figure 1: Nimbus IV satellite. The spacecraft is approximately 10 feet tall and 11 feet wide. The base of the satellite houses the sensor instrumentation and other electronic components. The two solar pads continually face the sun and convert solar energy to power the spacecraft. (NASA photo)



223 222 221 220 219 218 217 216 215 214 213 212

Figure 2: Montage of Nimbus III HRIR Daytime (30 April 1969) photofacsimile strips showing global cloud cover and continent configurations. (All Nimbus pictures were furnished by the NASA Nimbus Project, Goddard Space Flight Center, Greenbelt, Maryland.)

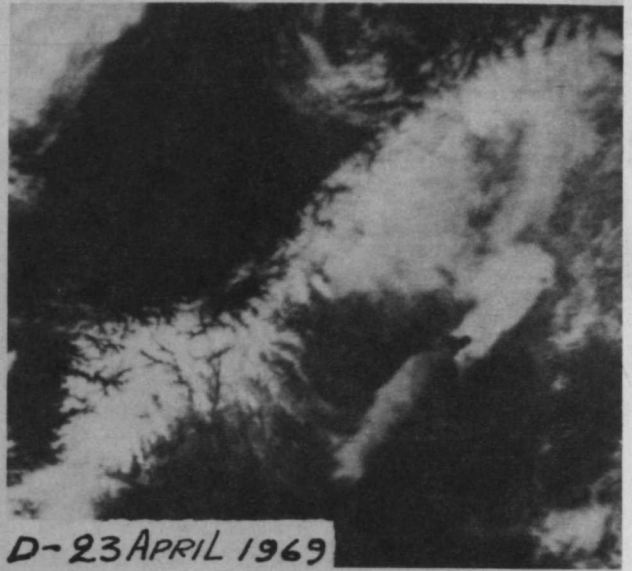
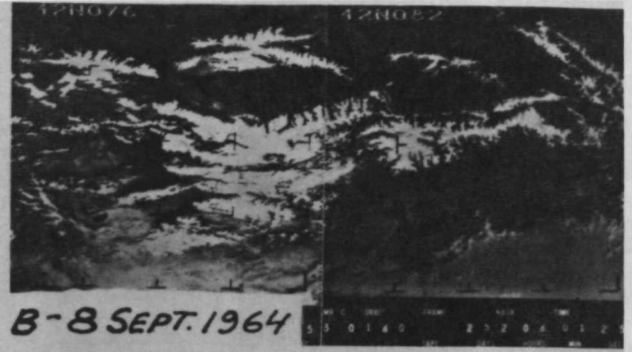
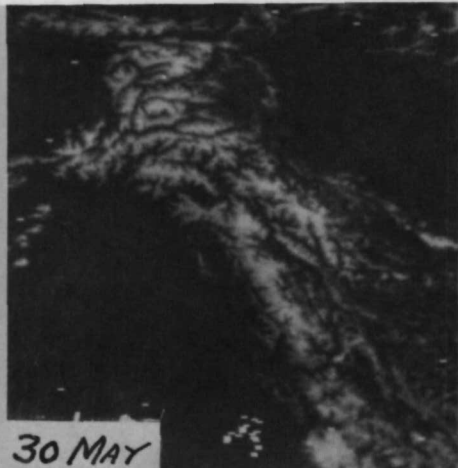


Figure 3: See next page for explanations.



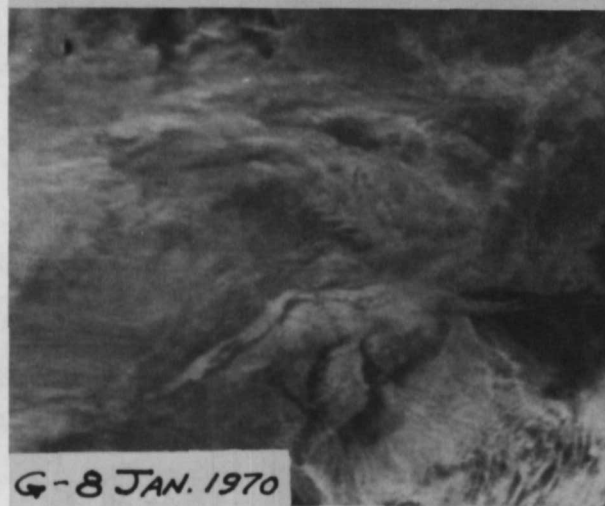
F-28 APRIL 1969



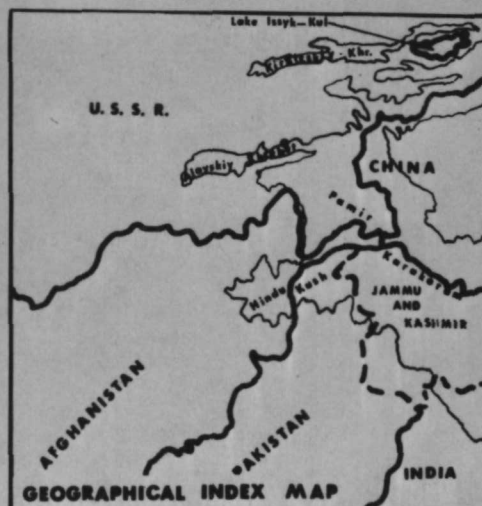
30 MAY



21 JUNE



G-8 JAN. 1970



GEOGRAPHICAL INDEX MAP



18 JULY

Figure 3: Snow and ice cover distribution viewed by Nimbus satellites: A - Nimbus I AVCS photograph, Ellsemere Island; B - Nimbus I AVCS, Lake Issyk-Kul, Kirgiz U.S.S.R.; C - Nimbus II APT, northwest coast of U.S.A. and southwestern Canada; D and E - Nimbus III and IV IDCS respectively, Scandinavia; F - Nimbus III temporal sequence of IDCS pictures, see map insert for geographical location; G - Nimbus III IDCS, fresh one-half foot snowfall covered a belt from the Blue Ridge Mountains, northeast through eastern Pennsylvania, to northern New Jersey. The remainder of the northeast United States is still covered by the remains of a Christmas snowfall.

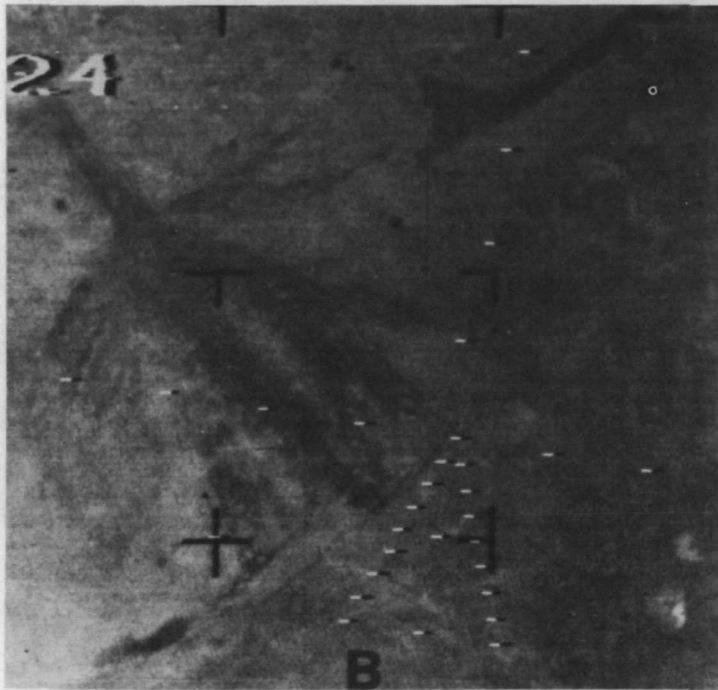
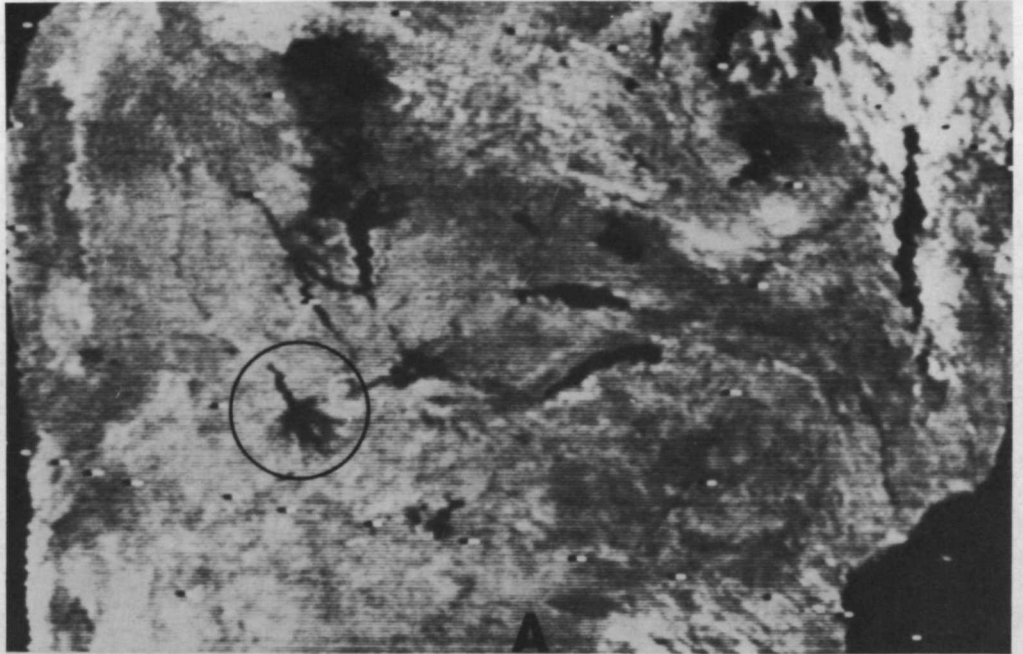
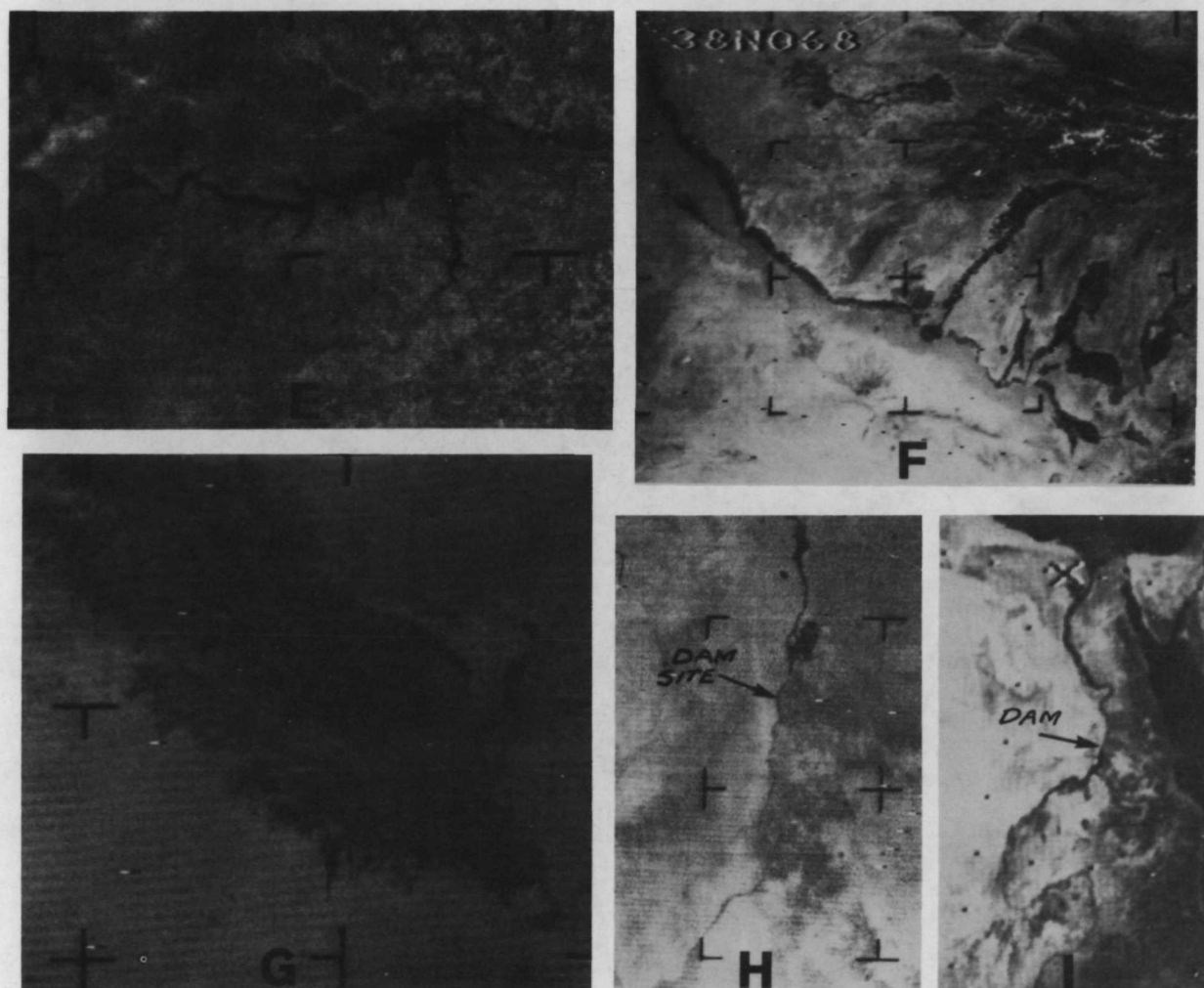


Figure 4: See next page for explanation.



**Figure 4:** Drainage systems, lakes and reservoirs viewed by Nimbus satellites: A - Nimbus III HRIR (Day), South Africa (Zambezi watershed). The Okavango Basin (circled) is illustrated in B; B - Nimbus I AVCS, Okavango Basin, South Africa; C - Great Salt Lake and Great Salt Lake Desert, Utah (10 September 1964); D - Lake Mead, Nevada (2 September 1964); E - Fort Peck Reservoir, Montana (17 September 1964); F - Nimbus I AVCS, Amu Dary'a River, its tributaries and oases, U.S.S.R. and Afghanistan border area; G - Nimbus I AVCS, Kara Kum Desert, marsh and irrigated cropland along the Amu Dary'a River Delta, U.S.S.R.; H and I - Nimbus I AVCS and Nimbus III HRIR respectively. Arrows point to the site of the Aswan Dam, Egypt. H - Construction of dam four years under way; I - Dam after one year in operation.

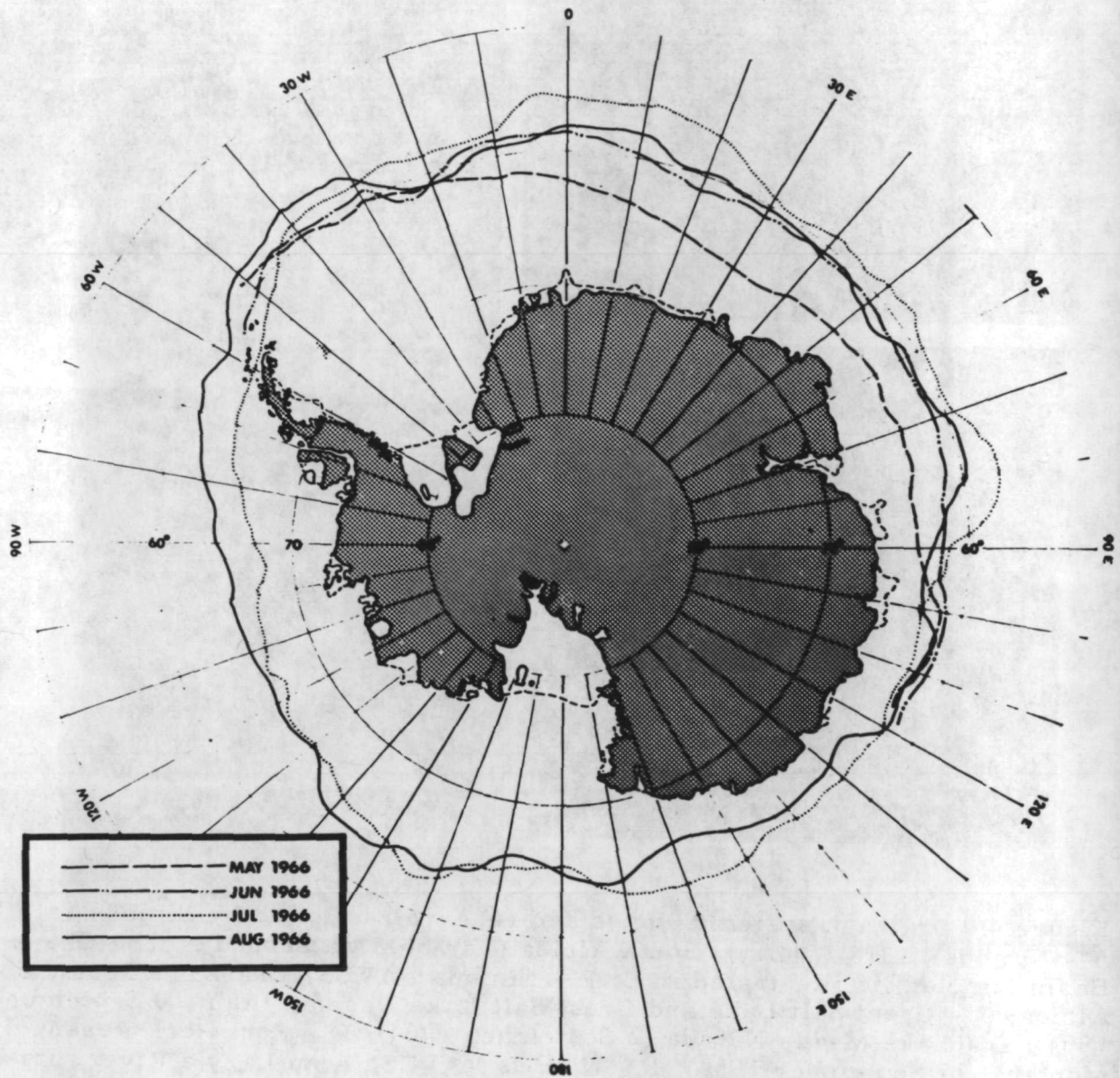


Figure 5: Average monthly Antarctic Pack Ice boundaries derived from Nimbus II AVCS data.

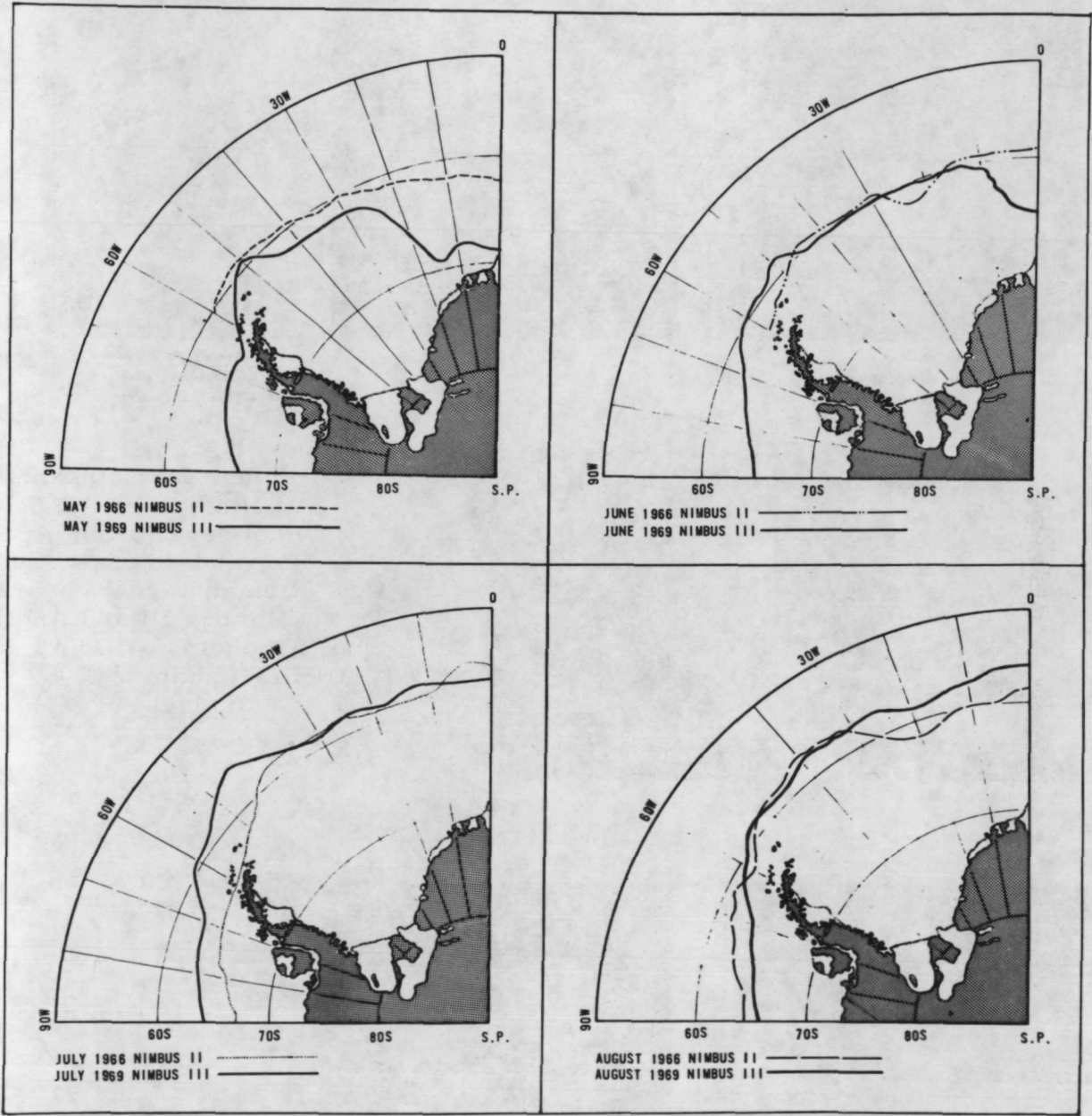
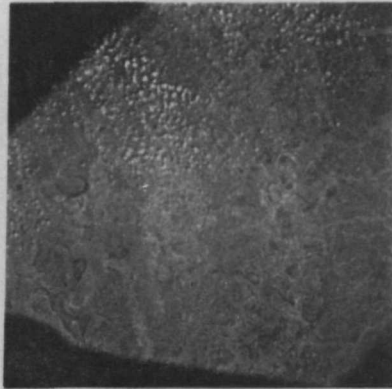
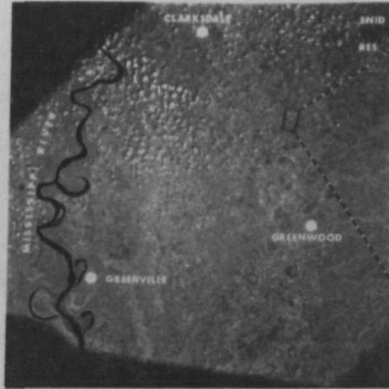


Figure 6: A comparison of monthly fluctuations in the Antarctic Pack Ice boundaries observed by Nimbus II (AVCS) and Nimbus III (IDCS) satellites.



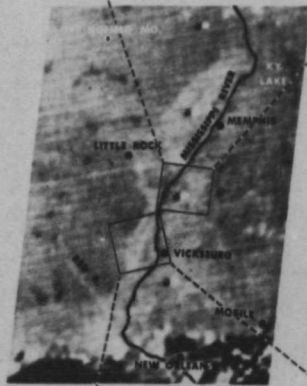
**APOLLO IX**  
**11 MARCH 1969**  
**RESOLUTION: 170 FT.**



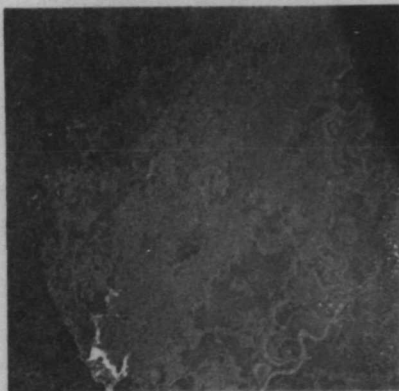
**AIRCRAFT PHOTOGRAPH**  
**21 SEPTEMBER 1962**  
**RESOLUTION: .5 FT.**



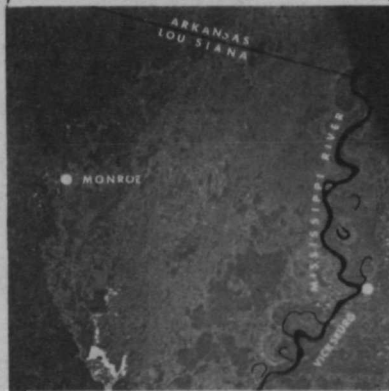
**NIMBUS III HRIR (D)**  
**9 AUGUST 1969**  
**RESOLUTION: 5 n. mi.**

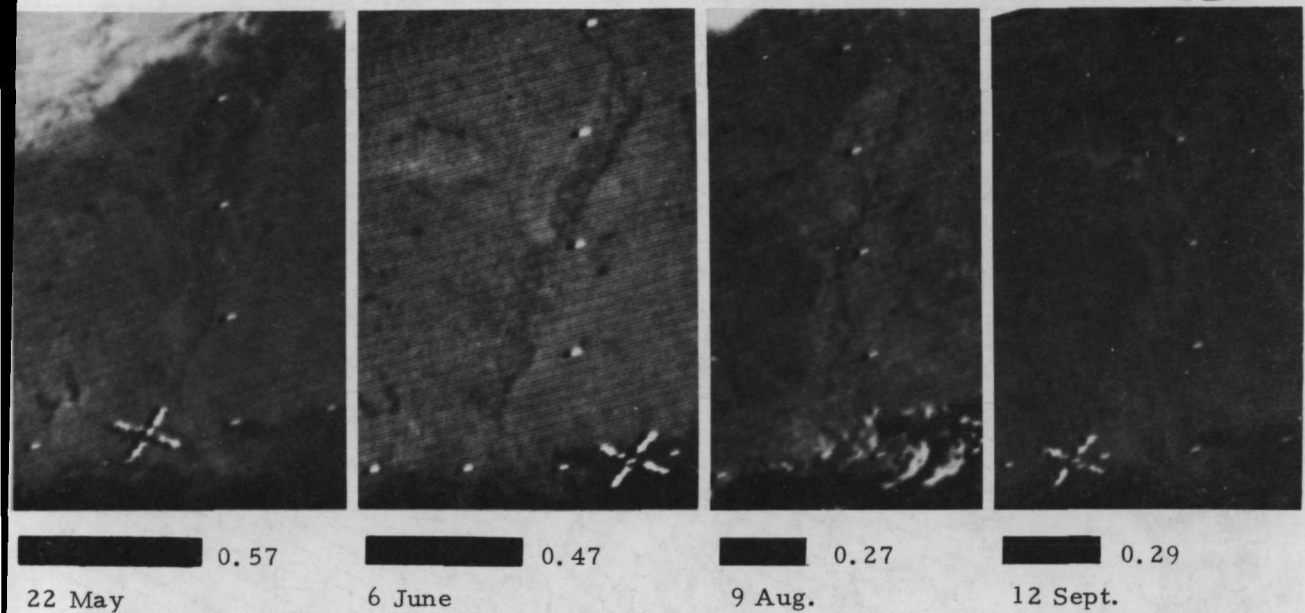


**Figure 7: Comparison of Nimbus III (HRIR photofacsimile), Apollo IX, and aircraft resolution and areal coverage (Nimbus III and Apollo IX photos - NASA, aircraft photo - U. S. Geological Survey)**

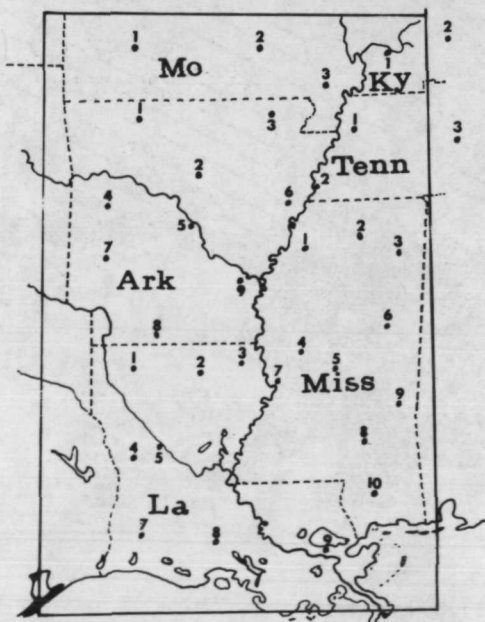


**APOLLO IX**  
**9 MARCH 1969**  
**RESOLUTION: 170 FT.**





Horizontal bars represent rainfall averages in inches for the week prior to image acquisition. 22 May - rainfall of 0.5 to 2 inches on 18 May; 6 June - rainfall 0.2 to 1.2 inches in Louisiana and Mississippi on 2 June. Light and scattered rainfall elsewhere since 22 May; 9 August - almost no rainfall since 28 July; 12 September - generally heavy rainfall 1 through 12 September. No rainfall from 9 through 12 September (43).



Index map of the imaged area. Numbers represent rainfall gauging station from which information was collected.

#### ARKANSAS

1. Harrison
2. Greers Ferry
3. Walnut Ridge
4. Blue Mts. Dam
5. Little Rock
6. Forrest City
7. Narrows Dam
8. El Dorado
9. Dumas

#### KENTUCKY

1. Paducah
2. Madisonville

#### LOUISIANA

1. Minden
2. Calhoun Exp. Sta.
3. Epps 6 W
4. Leesville
5. Alexandria
6. Baton Rouge
7. Lake Charles
8. Lafayette
9. New Orleans

#### MISSISSIPPI

1. Clarksdale
2. University
3. Tupelo
4. Yazoo City
5. Canton
6. Louisville
7. Vicksburg
8. Collins
9. Meridian
10. Wiggins

#### MISSOURI

1. Springfield
2. Ellington
3. Malden

#### TENNESSEE

1. Dyersburg
2. Memphis
3. Centerville

Gauging stations from which rainfall information was collected.

**Figure 8:** The varying tonal changes in the Mississippi River Valley illustrated here correspond to solar reflectance recorded by the Nimbus III radiometer (Daytime HRIR) in the 0.7 to 1.3 micron band.

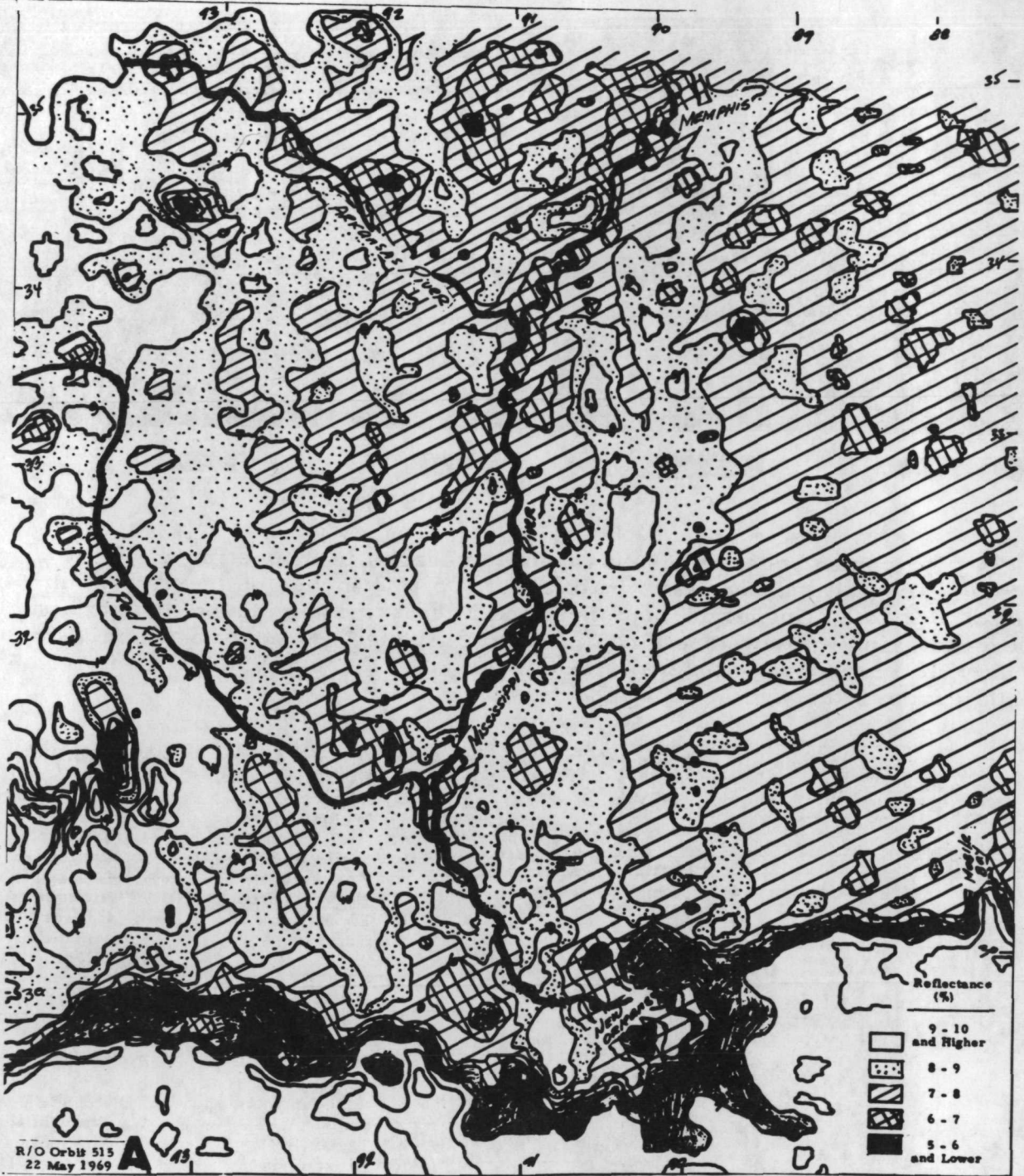


Figure 9: Computer produced (Nimbus III HRIR daytime, 0.7 - 1.3 micron band) maps showing Mississippi River Valley reflectance values. These maps are a digitized product from specially processed analog signals shown pictorially in Figure 8. Such maps are used for more comprehensive analyses of terrestrial features imaged by the Nimbus radiometers. Original scale of grid print map, 1:1 million (Mercator), contoured at 1% interval.

A. Nimbus III HRIR (Day) readout orbit 515, 22 May 1969. Reflectance values along the Mississippi River Valley are lower (6-8%) than on Map B.



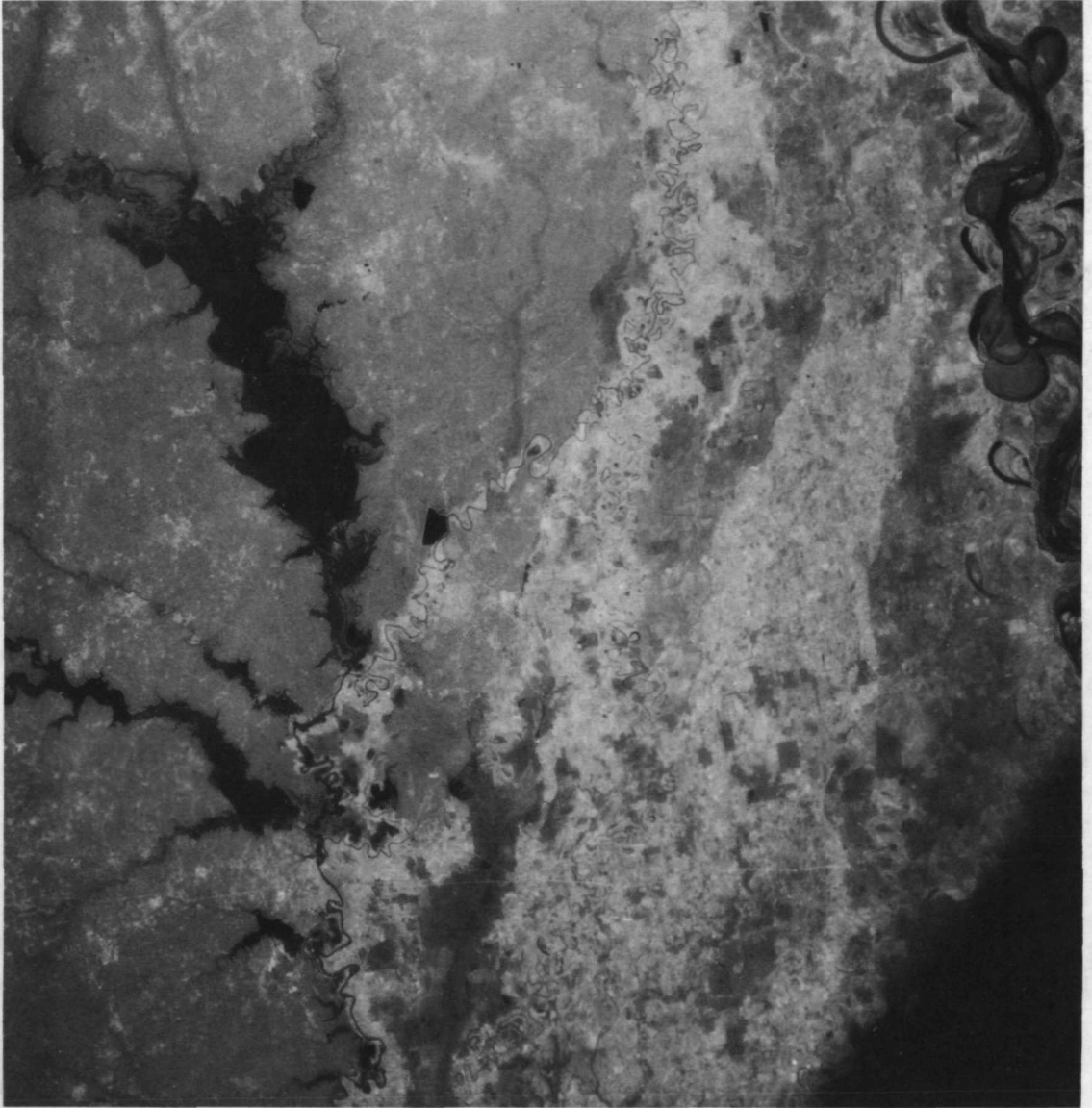


Figure 10: Apollo IX photograph of the lower Mississippi Valley taken on 9 March 1969. The flooded Ouachita River is in the upper left hand portion of the picture. The highly cultivated flood plains of the Mississippi River occupies the right hand portion of the photograph.

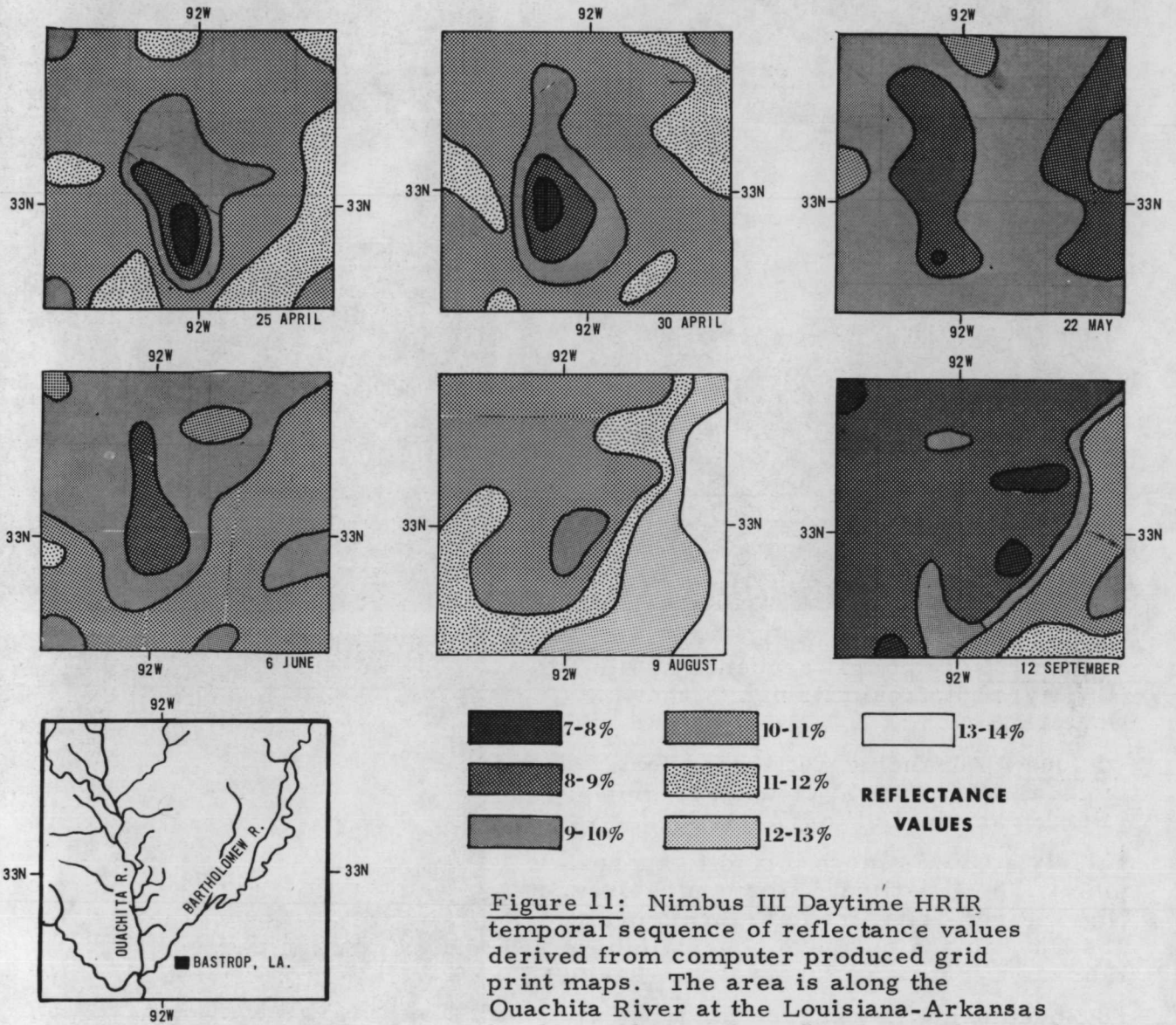


Figure 11: Nimbus III Daytime HRIR temporal sequence of reflectance values derived from computer produced grid print maps. The area is along the Ouachita River at the Louisiana-Arkansas border. Changes in reflectance values and pattern along the Ouachita correlate with lingering effects of an early spring flood. Some of the other patterns correlate with soil and vegetation patterns.



**Figure 12:** Temporal sequence of Nimbus III (Day) photofacsimile prints showing western Africa.

**16 June** - Advancing wet season for tropical West Africa; clouds are moving inland from the Gulf of Guinea.

**13 July** - Clouds move inland to approximately  $15^{\circ}$  N latitude; storm gyre over Niger River delta; frontal storms over Jos Plateau and northern Nigeria (above Komadiya-Yube and Sokota River Basins).

**18 November** - Dry season for tropical West Africa. Dust and haze of the harmattan to altitudes of 8-12,000 feet over the Niger River Basin and northern Nigeria.



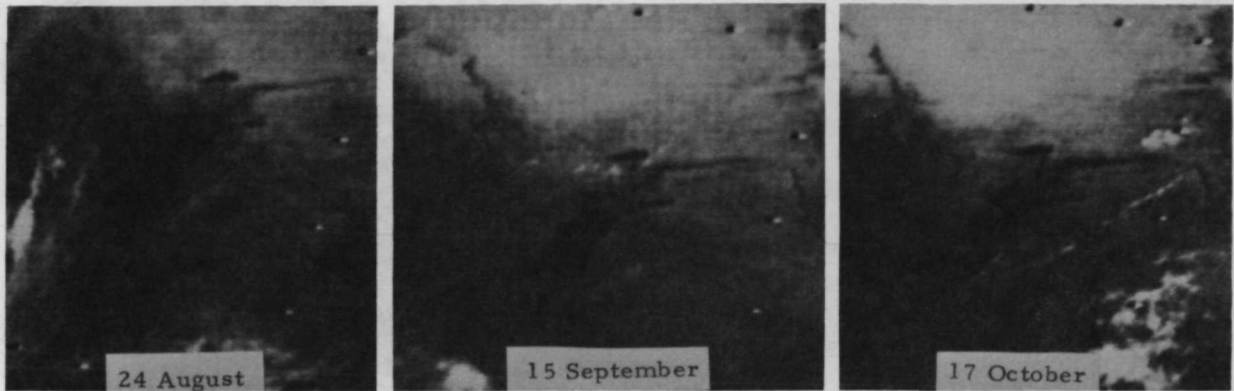
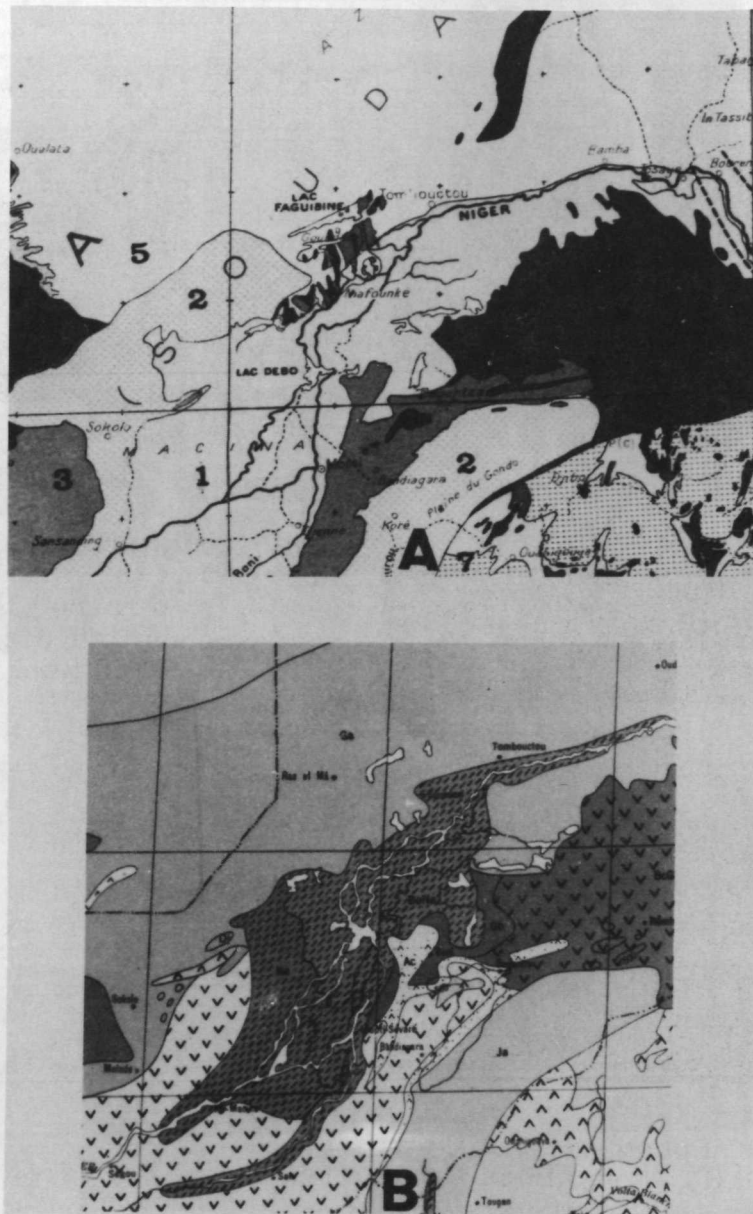


Figure 13: Temporal sequence of Nimbus III HRIR (Day) photofacsimile prints illustrating the changing tones of the inland "delta" region from August to October corresponds to hydrologic and vegetative conditions on the ground.



Figure 14: Gemini VI photo of the Niger River Valley in central Mali, West Africa. The long dart above and to the right of the striated areas is Lake Faguibine; Lake Haribongo is approximately 100 statute miles below and to the left of it. The city of Timbuktu is between Lake Faguibine and the river. The dark linear pattern south of the river is the result of flooding of stabilized sand dunes. The El Djouf Desert (Sahara) at the upper right is separated from the Auouker Hodh Basin to the west by a cuesta (44). (NASA photo, S65-63247, December 16, 1963)



**Figure 15:** Geologic and Soil Maps of Niger River Valley South of Timbuktu, Central Mali, West Africa.

**A - Geologic Map (45):** 1. Quaternary Sediments, 2. Tertiary Sediments, 3. and 4. Pre-Cambrian Lithology, 5. Sands and Dunes, 6. Basic Intrusives, 7. Granites and Pre-Cambrian Lithologies.

**B - Soil Map (41):** Na - Mineral Hydromorphic Soils, Bo - Riverine and Lacustrine Alluvium, Ga - Sands, Bc - Ferruginous Crusts.

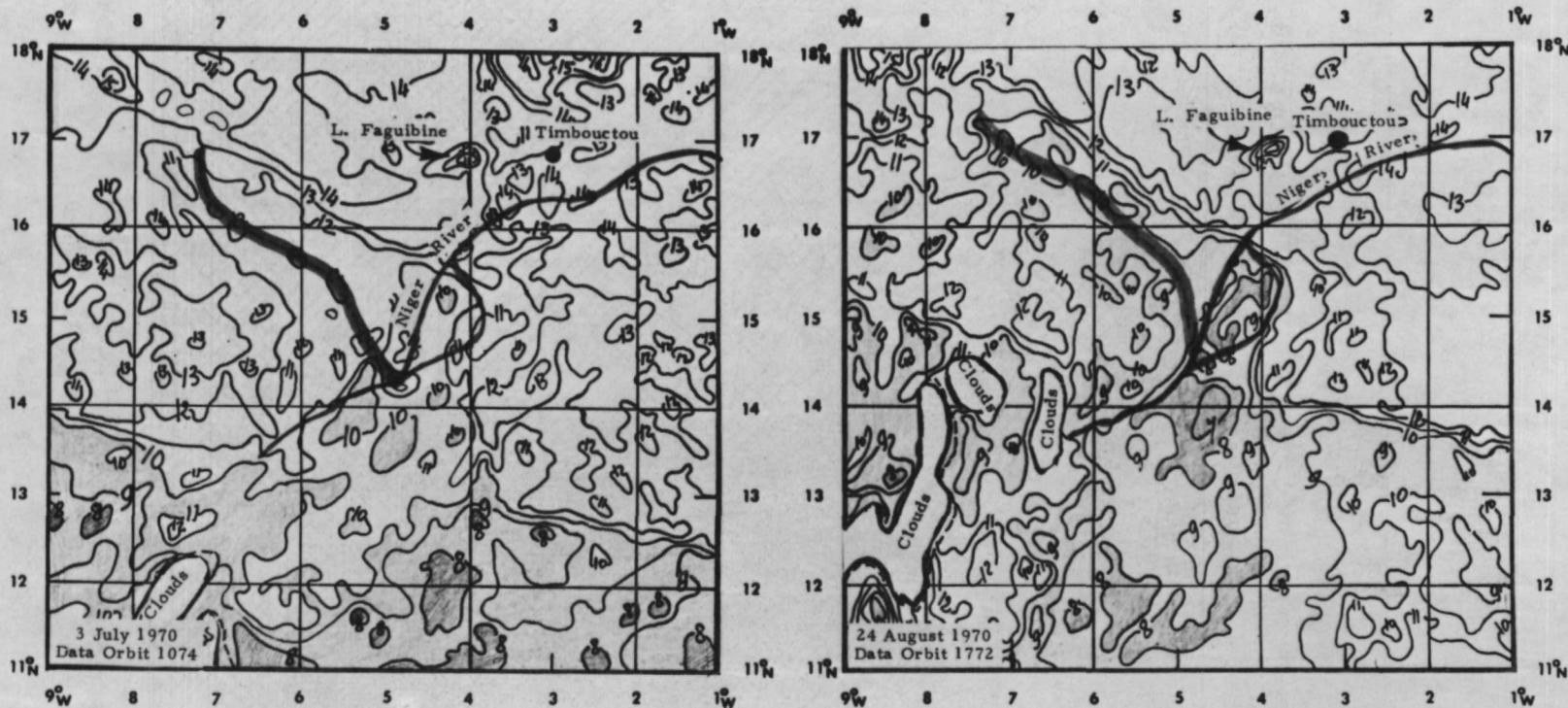


Figure 16: Nimbus III HRIR Daytime Reflectance Values (0.7 - 1.3 spectral band), Central Mali, Africa. Reflectance values lower than 10% are shaded and are indicative of higher soil moisture content and vegetative cover.

Projected former course (Pre-Pleistocene) of the Niger River is accentuated by the heavy shaded line, trending in the NW-SE direction.

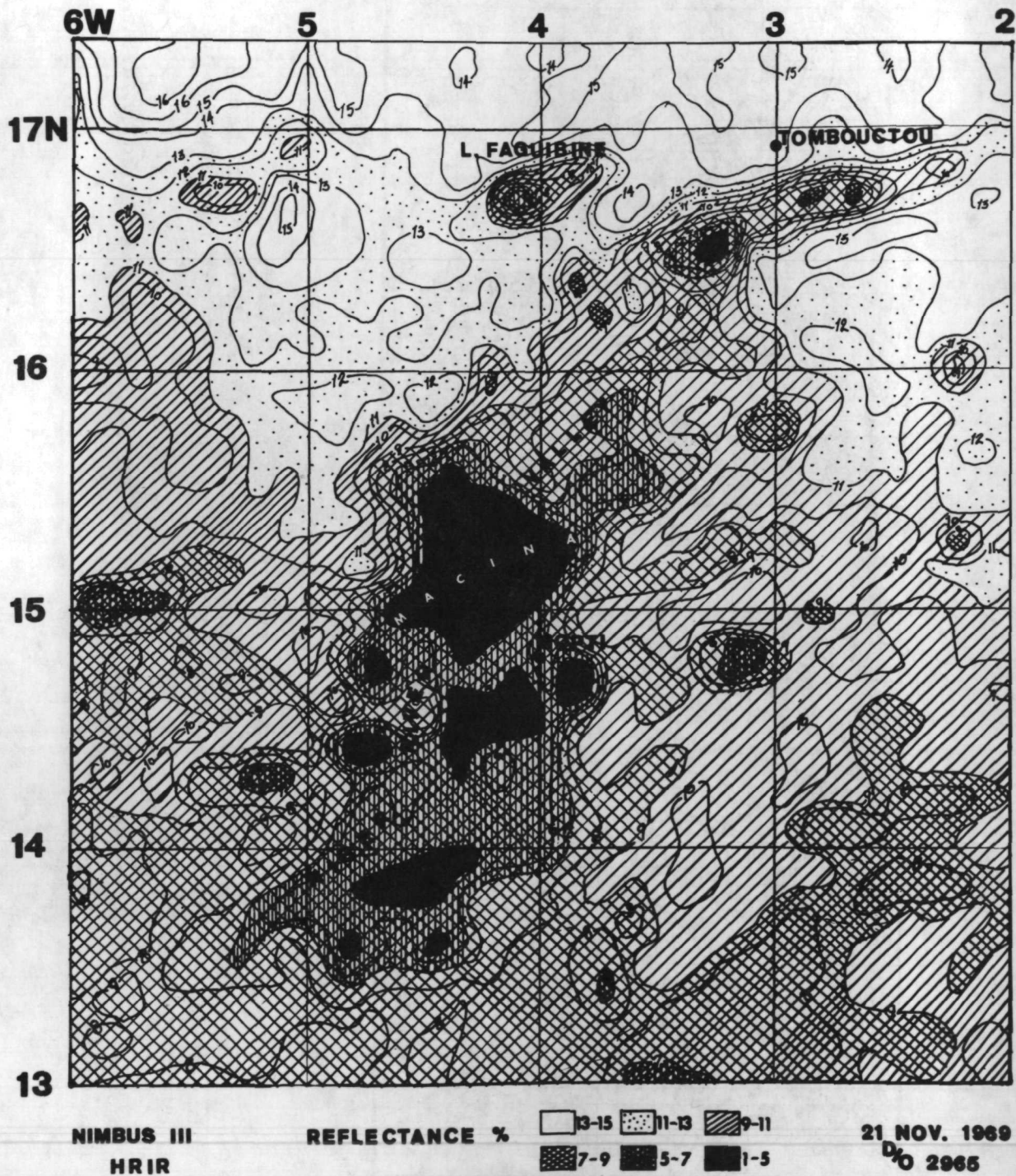


Figure 17: See page 511 for explanation.

Figure 17: Distribution of reflectance values and patterns in the Upper Niger River Valley, Africa, recorded by the Nimbus III HRIR radiometer in the 0.7 - 1.3 spectral band. November in Central Mali is the end of the rainy season ("hivernage") and the beginning of the dry season. The low regional reflectances (compared to July and August maps, Figure 13) are due to the moisture stored in the ground during the wet season, increased evapotranspiration, and the vegetal cover (aquatic and land) that is at its maximum during this season. Reflectance values on this map correspond approximately to the following terrestrial features: 15% and higher: clouds; 12-15%: desert sands (loose material); 11-13%: mostly bare ground (relatively compact); 9-11%: lateritic soil with sparse vegetation; 7-9%: savannah grasslands; 5-7%: vegetation and moisture-saturated flood plain soil; 1-5%: surface water, heavy vegetation, and water-laden ferruginous ground.